JOURNAL OF PROPULSION AND POWER
Vol. 21, No. 6, November–December 2005

Ignition and Oxidation of Ethylene-Oxygen-Diluent Mixtures with and Without Silane

Danielle M. Kalitan*
The Aerospace Corporation, El Segundo, California 90245
and
Joel M. Hall† and Eric L. Petersen‡
University of Central Florida, Orlando, Florida 32816

Several dilute mixtures of varying concentrations and equivalence ratios ($\phi = 0.5, 1.0$) of $C_2H_4/O_2/Ar/SiH_4$ were studied between 1115–1900 K and 0.9–3.3 atm. Argon dilution ranged from 96–98% with total concentrations between 0.67 and 3.2×10^{-5} mol/cm^3. Reaction progress was monitored using chemiluminescence emission from the hydroxyl radical near 307 nm. For SiH_4 concentrations less than 10% of the ethylene in the mixture by volume, the ignition delay time was reduced by approximately 30% to greater than 50%. The addition of SiH_4 had a small effect on ignition activation energy, indicating the chain branching mechanism for C_2H_4 ignition is sped up but not altered greatly by the silane at higher temperatures. After adding an appropriate OH* submechanism, several modern kinetics mechanisms containing high-temperature ethylene chemistry were compared to the data without SiH_4. Most of the mechanisms captured the ignition activation energy quite well, but only the mechanism of Wang and Laskin (1998) was typically within 10% of the absolute experimental ignition times over the entire range of conditions. The basic formation and quenching characteristics of the OH* profiles were reproduced by most mechanisms, but each requires some improvement to match all features.

Introduction

ETHYLENE combustion and chemical kinetics are of interest to high-speed propulsion, materials synthesis, and many other applications because C_2H_4 is a key fuel and an important intermediate in the oxidation of higher-order hydrocarbons. Numerous studies have been conducted starting in the late 1960s and ranging to the present day.[1–21] One parameter of interest in the oxidation of C_2H_4 is its ignition delay time τ_{ign}. Ignition-time measurements are not only of practical interest but also of fundamental interest because such data are commonly used to validate detailed chemical kinetics mechanisms. High-temperature τ_{ign} data are usually obtained using the shock-tube technique. A survey of shock-tube ignition data for lower-order hydrocarbons can be found in Schultz and Shepherd,[15] and a recent survey specific to ethylene ignition in shock tubes is provided by Varatharajan and Williams.[19]

With ever more precise methods of measuring reaction rates and species time histories, coupled with more powerful methods of conducting numerical analysis for comparison to experimental data, the study of ethylene chemical kinetics is becoming more complete. Even so, there is still much discrepancy among established ignition delay time data, and modern chemical kinetics mechanisms are inadequate over all ranges of temperature, pressure, and stoichiometry. For example, differences among τ_{ign} studies are attributed to differences in diagnostic technique, purity level, concentration ranges, temperature ranges, and definition of ignition time.[19] Many of these issues can be resolved using modern laboratory techniques and the correct interpretation of the data for an equivalent comparison to detailed kinetics models. New studies on ethylene ignition and oxidation are warranted based solely on these discrepancies. However, a primary focus of the present study, in addition to obtaining fundamental C_2H_4 ignition data, was the interaction between hydrocarbons and the oxidation of silane.

Silane oxidation has potential application in high-speed combustion and has been of interest since the landmark experiments of McLain et al.[22] Silane, hypergolic in the presence of oxygen, is applicable to aerospace applications for its ignition-enhancing capabilities.[23,24] Recent studies have shown the benefits of adding silane to the combustion process of common hydrocarbon fuels by reducing ignition delay times, resulting in shorter residence times in high-speed engines. Additionally, silane is used as a silicon precursor for the materials synthesis of nanoparticles and chemical vapor deposition.[25–29] A byproduct of the silane oxidation process is the formation of silicon oxides such as SiO and SiO_2, which are useful for the flame synthesis of glasses, coatings, and other materials. In such processes, the silane precursor is often added to a hydrocarbon-fueled reaction zone, and so the kinetics of the coupled hydrocarbon/SiH_4 oxidation process are important.[25,30–32]

Over the past two decades, much progress has been made on the formation of a chemical kinetics mechanism for the oxidation of SiH_4 and related molecules, but there still exist considerable uncertainty and discrepancy on individual reactions and entire mechanisms, particularly those that can treat the formation of heterogeneous, Si-based compounds at flame temperatures.[33] The process is complicated further when in the presence of hydrocarbons, and few chemical kinetics studies exist for silane/C_xH_y oxidation.[25] To provide much-needed fundamental data in these areas, the authors have been conducting a series of shock-tube experiments and chemical kinetics analyses of silane ignition and oxidation. These previous efforts include the study of H_2-based mixtures[33,34] and mixtures based on methane[34] and acetylene.[35,36]

The present paper continues the study of high-temperature ($T > 1000$ K) hydrocarbon/silane combustion at near-atmospheric pressures by exploring ethylene-based mixtures with small quantities of SiH_4. Ignition delay times measured from shock-tube experiments with and without silane were conducted and are summarized. For the results without silane, comparisons are drawn between the

Presented as Paper 2004-1323 at the AIAA 42nd Aerospace Sciences Meeting and Exhibit, Reno, NV, 5–8 January 2004; received 2 February 2004; revision received 21 April 2005; accepted for publication 22 April 2005.

*Member of the Technical Staff, Space Materials Laboratory; currently Associate Member of the Technical Staff, P.O. Box 92957-M5/754, Propulsion Science and Experimental Mechanics, Los Angeles, CA 90009-2957.

†Research Assistant, Mechanical, Materials and Aerospace Engineering. Student Member AIAA.

‡Assistant Professor, Mechanical, Materials and Aerospace Engineering. Senior Member AIAA.

Table 1 List of test mixtures, their compositions, and test ranges

Mixture	$\%C_2H_4$	$\%O_2$	%Ar	$\%SiH_4$	ϕ	[M] $\times 10^5$, mol/cm^3	T, K[a]	E, kcal/mol
1	1.00	3.00	96.000	0.000	1.0	0.71–1.2	1286–1683	22.8
2	0.50	1.50	98.000	0.000	1.0	0.67–1.1	1223–1733	24.9
3	0.50	1.50	97.964	0.036	1.0	0.81–1.1	1274–1579	28.9
4	1.00	3.00	95.978	0.022	1.0	0.81–1.2	1190–1539	25.7
5	0.30	1.70	98.000	0.000	0.5	0.80–1.2	1314–1525	23.2
6	0.29	1.71	97.964	0.036	0.5	0.71–1.3	1320–1901	21.2
7	0.57	3.43	96.000	0.000	0.5	0.7–1.3	1244–1754	20.1
Overall, no SiH_4	——	——	——	——	——	0.67–3.0	1223–1746	26.6
Overall, w/SiH_4	——	——	——	——	——	7.1–1.3	1190–1901	26.3

[a]The temperature range corresponds to the range of validity for the activation energies E.

measured ignition delay time data and the results of previous experimental studies. For completeness, the experimental results without SiH_4 are compared to state-of-the-art chemical kinetics models to discern the abilities of these models to reproduce the data over the range of conditions herein. Also, the combination of ethylene combustion with silane addition was studied, and some results are described.

Experiment

Apparatus

All experiments were conducted in the shock-tube facility at The Aerospace Corporation. Details concerning the physical layout of the apparatus as well as descriptions of the auxiliary components and diagnostics not described herein can be found in Petersen et al.[37] The helium-driven shock tube has a driven section diameter of 16.2 cm and a driven length of 10.7 m. The conditions behind the reflected shock wave immediately on reflection from the endwall were determined from the measured incident shock-wave speed and the standard, one-dimensional shock-wave relations. The shock velocity on reaching the endwall was determined by fitting a line to the four different axial-velocity measurements and extrapolating to the endwall.[37] Uncertainty in the test temperature using this technique in the present facility is less than 10 K.

Seven mixtures of $C_2H_4/O_2/Ar$ with and without silane were examined. Table 1 lists the various mixtures and their corresponding fuel-to-oxidizer equivalence ratios ϕ. The mixtures were prepared in a stainless-steel mixing vessel. To obtain the correct mixture ratios, the partial pressure method was employed. The gases used were ultra-high-purity (UHP) argon, UHP O_2, research-grade C_2H_4, and research-grade SiH_4. The mixtures containing both SiH_4 and O_2, because of their hypergolic nature, were specially premixed using the technique demonstrated previously.[34]

Light emission from $OH^* A^2\Sigma^+ \rightarrow X^2\Pi$ chemiluminescence was collected through two CaF_2 windows, one located at the endwall and the other located 1.6 cm from the endwall. Two Hamamatsu 1P21 photomultiplier tubes (PMT) in specially designed housings, one at each CaF_2 window, were used with 310-nm (10-nm full width at half maximum) filters to measure the ultraviolet OH^* emission. The light detected by the sidewall PMT was passed through a narrow ($\approx$1 mm) slit to ensure adequate time resolution for OH^* profiles. Also, the PMT circuitry was optimized to maintain good signal-to-noise, time response, and linearity. Fast-response pressure transducers were colocated at both window positions and were needed to monitor the arrival of the reflected shock wave. Because of the highly dilute mixtures (Table 1), pressure was not used as an ignition diagnostic because the corresponding increase in pressure caused by ignition was either not observed or was not strong enough to determine an ignition time with acceptable precision.

Data Analysis

With regard to some of the discrepancies among different ignition delay time studies just mentioned, the diagnostic details and the interpretation of the measured results must be considered carefully. The details of the data reduction must then be relayed to others so that future use of the data to validate chemical kinetics models and

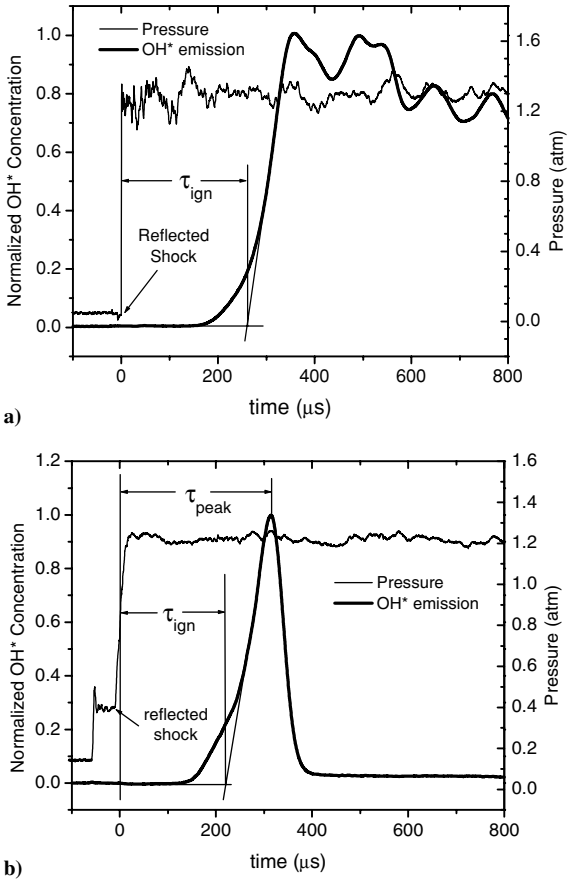

Fig. 1 Characteristic times defined with results of a typical experiment: a) endwall and b) sidewall, mixture 5, $\phi = 0.5$, 1404 K, 1.23 atm.

to compare with existing data are consistent with the experimental study (or at least any differences that remain are identified). Figure 1 defines two characteristic times, τ_{ign} and time-to-peak concentration τ_{peak}.

For the endwall emission data, Fig. 1a shows that the ignition time is defined as the intersection between a line corresponding to the maximum slope and the initial concentration. The authors have found that such as definition tends to agree with similar definitions from older data employing pressure as a diagnostic and other species, but can still be species specific (see the following).[34,36] The corresponding sidewall emission trace is shown in Fig. 1b. Peak time, although good for validating kinetics models, does not make a good ignition delay time because it tends to be too species specific.[36]

As shown in Fig. 1, the endwall emission trace is not the same as the sidewall emission trace in appearance because of differences in the optical path and the transient nature of shock-tube experiments. It is commonly accepted that the endwall emission trace gives the true ignition delay time because the gas molecules near the endwall are exposed to the reflected shock wave before molecules further

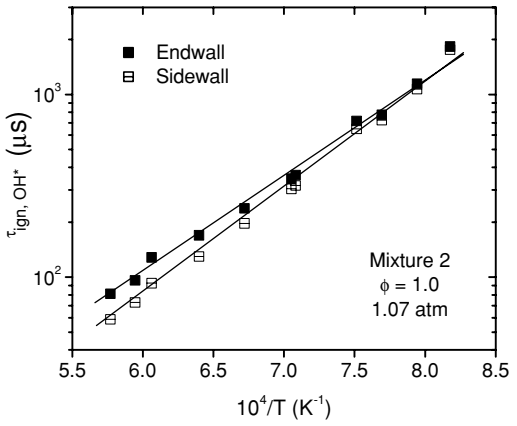

Fig. 2 Comparison of ignition delay times obtained from endwall and sidewall emission traces.

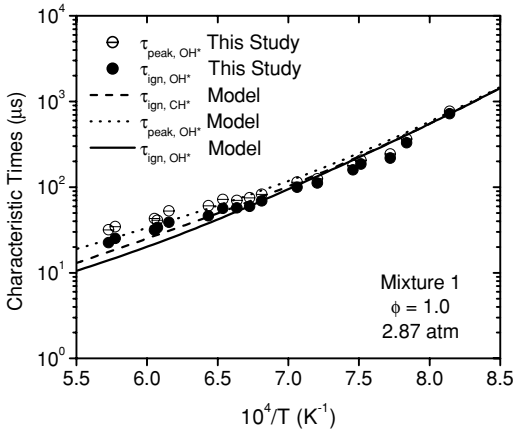

Fig. 3 Different characteristic time definitions from the data of mixture 1 (τ_{ign,OH^*} and τ_{peak,OH^*}) and the kinetics model of Wang and Laskin[40] (also, data available online at http://ame-www.usc.edu/research/combustion/combustionkinetics/c2_download.html.) (τ_{ign,OH^*}, τ_{ign,CH^*}, and τ_{peak,OH^*}). Peak times are generally longer than ignition times, and τ_{ign} from OH^* and CH^* differ slightly but are within the precision of the data.

away, as at the sidewall port, and are immune to potential nonideal gas dynamic effects because of ignition-induced motion of the gas. Ideally, both measurements should produce the same ignition delay times, but nonideal gas dynamic effects caused by the ignition process itself cause the sidewall ignition to appear accelerated because of an "ignition wave" that moves from the endwall. This phenomenon is well known in cases of strong ignition, which occurs in highly exothermic mixtures (i.e., mixtures with lower levels of dilution) and is discussed in Petersen et al.[38] and Horning et al.[39]

Although it was believed that dilution levels greater than about 95% are immune to such gas dynamic effects,[39] they were still observed in the ethylene experiments. Figure 2 shows typical results of τ_{ign} obtained simultaneously from both the endwall and the sidewall for a series of experiments using mixture 2 with a 98% argon dilution, the most diluted mixture herein. The sidewall ignition is accelerated slightly for the higher temperatures and can be as much as 30% faster than the endwall result. For temperatures less than about 1500 K, the differences were less than 10%. Similar results were observed for all mixtures. Therefore, because the endwall ignition is unaffected by such postignition gas dynamic effects, τ_{ign} is derived from endwall emission unless otherwise specified.

Nevertheless, species time histories obtained from the sidewall are useful for comparison to concentration profiles obtained from zero-dimensional chemical kinetics modeling. As seen in Fig. 1a, the endwall emission is only good for observing the initial ignition delay time. This fact is because the signal that reaches the detector at later times (because of the optical path that the detector "sees") is actually an integrated light signal from subsequent ignition occurring at locations away from the endwall; these locations further away were processed by the reflected shock wave at times later than the initial reflection from the endwall. Hence, ignition occurs later at these locations, producing seemingly continuous light emission that is picked up by the endwall detector and appears as "noise".

In contrast, the sidewall signal ideally only sees the same gas particles for the entire post-reflected shock test time, as in the zero-dimensional approximation. Characteristics other than τ_{ign}, such as τ_{peak}, can therefore be discerned from the sidewall measurement. However, a slight adjustment in time should be done to the sidewall trace to account for the nonideal gas dynamic effects caused by ignition, as already mentioned. The authors suggest adding the difference between endwall and sidewall ignition delay time (i.e., $\tau_{ign,endwall} - \tau_{ign,sidewall}$) to the time coordinates of the concentration time history when using the sidewall data in a quantitative comparison with chemical kinetics models (or with other experiments).

In summary, the endwall OH^* measurements are useful for τ_{ign}, whereas the sidewall measurements are useful for comparison with kinetics models and to provide details such as τ_{peak}. Because τ_{peak} is not measured at the endwall, the difference between the peak time and ignition from the sidewall (i.e., $\tau_{peak} - \tau_{ign}$) is provided herein. According to the zero-dimensional assumption that applies after ignition occurs at the sidewall, this difference should be the same as what would be measured at the endwall if that were possible.

Additional considerations when reducing the experimental data include the actual definition of ignition delay time. This detail can be quite important, particularly when comparing the data to the results of other experiments or modeling results that might be based on different diagnostics and different definitions of ignition time. For example, species that are often measured in shock-tube oxidation experiments include not only OH^* chemiluminescence, but CH^* chemiluminescence, ground-state OH, CO, CO_2, and several other species (and of course pressure). Ignition has been defined in many ways in the literature, including that in Fig. 1 as well as the peak concentration, the maximum derivative, and other prominent features.[19,36]

Shown in Fig. 3 is a comparison between τ_{ign,OH^*} and τ_{peak,OH^*} from the present experiments along with predictions from a chemical kinetics model for both as well as for τ_{ign} based on CH^*. (Details on the kinetics modeling are provided in a later section.) The time-to-peak OH^* tends to occur noticeably later than τ_{ign} as defined in Fig. 1b, a result that is corroborated by the modeling predictions. The authors have also found that τ_{ign,OH^*} tends to agree quite well with τ_{ign,CH^*},[36] also seen in Fig. 3. With these subtleties in mind, care should be exercised when using the ignition-time results of the present study (or any other study) for comparisons with other ignition data and with chemical kinetics models.

Results

Table 2 lists the characteristic times and corresponding temperatures and pressures for each mixture. Experimental reflected-shock temperatures and pressures ranged from 1115 to 1900 K and from 0.9 to 3.3 atm, respectively. The total concentration ranged from 6.7×10^{-6} to 3.2×10^{-5} mol/cm^3. As just discussed, the peak times are presented as relative times (i.e., $\tau_{peak} - \tau_{ign}$). The worst-case uncertainty in the stated ignition delay times is approximately 20% of the values listed, although in most cases the uncertainty is much less than 20% and typically on the order of 5–10%. Presented next is a comparison of the data to previous studies, plots of the species time histories, and ignition delay time graphs for the various mixtures.

Comparison to Previous Studies

Mixture 1 experiments were conducted at a pressure near 3 atm for the purpose of comparison to previous experimental tests run by Baker and Skinner[1] and Hidaka et al.[9] Baker and Skinner were among the first to complete a wide-scale analysis of ethylene ignition using a shock tube. Because of this, their data are often the most widely used for comparison and analysis purposes. For the current ethylene investigation, the Baker and Skinner[1] ignition-time

Table 2 Data table with corresponding run conditions, ignition delay times, and peak times relative to τ_{ign}, all defined at the endwall

Mixture	T, K	P, atm	τ_{ign}, μs	$\tau_{peak} - \tau_{ign}$, μs
1	1647	2.61	36	8
	1530	2.96	56	15
	1487	3.02	58	15
	1507	2.77	59	13
	1388	2.88	112	14
	1341	2.91	159	20
	1295	2.90	219	25
	1468	2.77	71	14
	1732	2.61	27	11
	1746	2.61	24	10
	1652	2.72	33	12
	1625	2.79	40	14
	1554	2.73	48	15
	1416	2.99	98	14
	1331	3.05	180	20
	1276	3.16	312	34
	1228	3.26	668	45
	1488	1.21	123	—
	1388	1.09	236	38
	1423	1.12	204	33
	1452	1.17	157	30
	1455	1.17	152	33
	1357	1.03	318	40
	1412	1.11	196	35
	1439	1.14	180	31
	1386	1.08	254	37
	1414	1.11	217	34
	1475	1.19	149	30
	1400	1.09	227	34
	1388	1.10	247	35
	1416	1.13	201	32
	1397	1.10	220	33
	1426	1.13	185	32
	1286	1.27	537	44
	1683	0.98	73	24
	1621	1.16	78	24
	1481	1.08	154	32
	1286	1.17	499	42
2	1597	2.60	52	10
	1495	2.72	114	36
	1278	3.02	621	92
	1389	2.94	206	52
	1259	1.18	1078.3	160
	1418	1.08	344.4	94
	1682	0.94	104.5	47
	1331	1.13	693	121
	1650	1.14	123.5	53
	1563	1.08	168.7	61
	1412	0.99	380.5	98
	1488	1.04	242.9	79
	1223	1.12	1544	106
	1300	1.10	762	125
	1223	1.12	1780	174
	1563	1.04	146	69
	1733	0.96	87	40
3	1274	1.20	591	135
	1333	1.13	387	117
	1434	1.09	208	104
	1527	1.01	104	76
	1579	1.07	70	69
	1544	1.13	87	70
	1534	1.15	101	75
	1517	1.16	96	67
	1362	1.07	336	125
	1453	1.19	155	82
4	1190	1.13	828	47
	1306	1.17	307	40
	1368	1.08	179	36
	1539	1.07	74	28
	1228	1.09	552	53
	1279	1.04	372	45
	1468	1.07	103	32
	1193	1.12	812	58
	1530	1.02	76	31
5	1343	1.30	361	104
	1461	1.12	202	80
	1525	1.00	160	63
	1404	1.23	270	83
	1314	1.16	529	134
	1330	1.28	396	105
6	1242	1.13	436	140
	1320	1.11	208	110
	1470	1.12	80	63
	1583	1.06	50	42
	1901	1.10	19	22
	1470	1.24	76	56
	1323	1.11	208	110
	1678	1.05	37	34
	1326	1.17	194	94
	1555	1.10	54	51
	1330	1.15	179	92
	1365	1.12	148	86
	1320	1.27	187	74
	1407	1.23	111	62
	1545	1.21	55	42
	1671	1.15	36	29
	1339	1.19	170	69
	1167	1.28	1265	218
	1531	1.12	59	53
7	1324	1.17	267	51
	1244	1.19	495	62
	1153	1.17	1740	169
	1158	1.22	1575	128
	1132	1.26	2539	121
	1129	1.3	2903	189
	1146	1.25	2070	156
	1302	1.18	389	49
	1308	1.38	383	46
	1284	1.34	384	47
	1339	1.33	257	34
	1271	1.23	485	55
	1214	1.27	938	71
	1158	1.22	1615	155
	1115	1.22	3397	369
	1147	1.23	2121	105
	1501	1.16	117	34
	1754	1.01	61	19

data were of interest as well as their activation energy value. Their correlation presented in Fig. 4 corresponds to their mixture that is equivalent to mixture 1 from Table 1.

Current results agree remarkably well with comparable studies when care is taken to compare similar diagnostics and ignition-time definitions. Differences in test pressure for data when plotted in the usual fashion as in Fig. 4 are a potential source of discrepancy when using results from previous investigators and in comparing the results of one study to another. In many cases, the test pressures for published data are not provided in any rigorous detail. For the comparison shown in Fig. 4, the data have been adjusted to a common pressure (2.9 atm) that is near the original experimental values of the two studies as well as the current one.

Also, to facilitate direct comparison of the present data to the two previous data sets that were based on sidewall measurements, the mixture 1 stoichiometric data in Fig. 4 are from the sidewall ignition measurements without corrections for gas dynamic effects. Note that Fig. 4 is the only plot wherein sidewall τ_{ign} values are used instead of endwall values.

The slight discrepancies seen in Fig. 4 can be caused by differences in diagnostics. Hidaka et al.[9] measured CH^* chemiluminescence (along with OH^* and C_2^*) through a window 1 cm from the endwall and defined τ_{ign} in a manner similar to that used herein. Baker and Skinner,[1] like the present study, recorded OH^* emission;

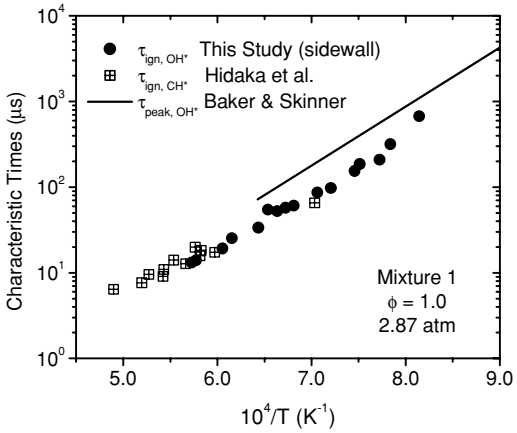

Fig. 4 Comparison of current results for mixture 1 with previous studies. All data are adjusted to the average pressure of the experiments, 2.87 atm.

however, they characterized ignition in terms of maximum emission intensity (τ_{peak}). As can be seen in Fig. 3, τ_{peak} occurs slightly later than does τ_{ign}, so that higher times for this parameter are to be expected.

As already mentioned, Fig. 3 also shows the results of the present study along with modeling predictions for the same conditions as Fig. 4. Modeling, based on the mechanism of Wang and Laskin,[40,§] suggests that some of the discrepancies might in fact be caused by different diagnostics. Specifically, the model shows τ_{ign,OH^*} occurring slightly faster than τ_{ign,CH^*} at higher temperatures (although the two are nearly identical at lower temperatures). Thus, in comparison to the Hidaka et al. data, which were measured for $1400 < T < 2050$ K, it is natural that the current results would be slightly faster, but such slight differences are nearly indiscernible within the precision of both sets of data.

The model also reveals that τ_{peak,OH^*} should be the slowest of the three times, with the difference discernable for $T > 1450$ K. This information is insufficient to explain the slower peak times found by Baker and Skinner,[1] however, because they measured colder shocks ($1110 < T < 1550$ K); over this temperature range, the differences among the three characteristic times are less than 10%. The differences with the Baker and Skinner data could also be caused by kinetics effects at intermediate temperatures ($T < 1250$ K) that tend to slow the onset of ignition.

Also noteworthy is the excellent agreement seen between the mechanism and the experiments in Fig. 3; this suggests that the model is valid and capable of providing valuable insight concerning the various species measured (see the following).

OH* Profiles

For each data point in Table 2, there is a corresponding OH* time history from the sidewall emission measurement. Summary plots are presented in this section to provide an overview of some of the key features and trends observed in the experiments. Each plot provides four concentration profiles from the same mixture at four different temperatures, and the concentrations are presented as raw voltages to stress the relative magnitudes (because the signal seen by the detector is linearly related to the OH* concentration). A calibration for absolute OH* concentrations was not available in the authors' laboratory during the time these data were taken. The four profiles shown in each plot in Fig. 5 are from the same detector setup and are therefore comparable.

Figure 5a presents typical profiles from the stoichiometric, less-diluted (96% Ar) mixture 1, and Fig. 5b presents the complementary mixture 4 containing silane. A typical trend includes the increase in OH* emission signal with temperature. Another trend is the presence of a slight increase in OH* long before the main ignition event, which becomes more noticeable at lower temperatures. This feature occurred in mixtures both with and without SiH_4. The accelerated ignition caused by the presence of silane is also seen when comparing profiles with similar temperatures between Figs. 5a and 5b.

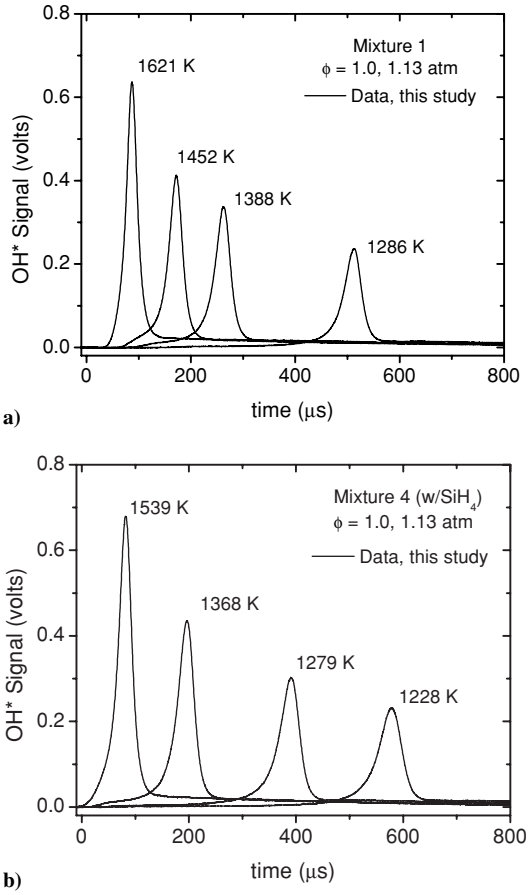

Fig. 5 Typical OH* time histories for higher-concentration stoichiometric mixtures (96% Ar): a) without silane (mixture 1) and b) with silane (mixture 4).

In higher-dilution $\phi = 1.0$ mixtures (98% Ar) without and with silane, the preignition OH* signal is more prominent than in the Fig. 5 plots, but the trends are otherwise similar to those seen in the less-diluted mixtures. The preignition OH* modulation was also present in the $\phi = 0.5$ mixtures, becoming more prominent at lower temperatures.

Ignition Delay Times

Presented in this section are ignition delay time plots on Arrhenius diagrams for each mixture, contrasting like mixtures with and without silane. Similar plots for τ_{peak} could also be presented, but the results are comparable in appearance to the τ_{ign} plots but larger in magnitude and are not included for brevity. In each set of data, the pressures are similar as seen in Table 2; however, the data displayed in each ignition delay time figure were adjusted to an average pressure for all points in the mixture set. This average pressure is displayed in each figure. The pressure dependence was taken from the overall ignition-time correlation (see the following).

Figure 6 displays the results for the stoichiometric mixtures with 96% argon dilution (mixtures 1 and 4) at an average pressure near 1 atm. As seen in the species profiles in Fig. 5, there is a reduction in ignition time with the addition of the silane, which for mixture 4 is 220 ppm, or about 2% of the fuel concentration. Even this small amount of SiH_4 generates a 40% reduction in τ_{ign} at higher temperatures and a 28% reduction at a temperature near 1280 K.

Even greater reductions in τ_{ign} are seen in Fig. 7 for the $\phi = 1.0$ mixtures with 98% argon dilution (mixtures 2 and 3). There is a 53% reduction at a temperature of 1600 K and a 38% reduction near

§Data available online at http://ame-www.usc.edu/research/combustion/combustionkinetics/c2_download.html.

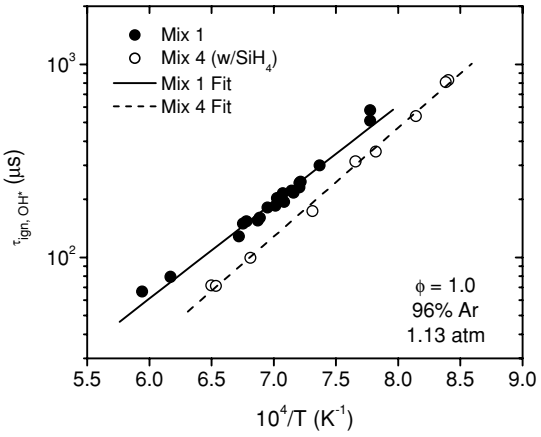

Fig. 6 Measured ignition delay times for higher-concentration $\phi = 1.0$ mixtures (96% Ar) with and without silane.

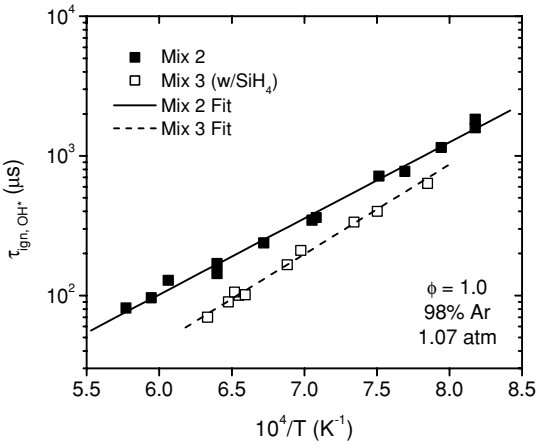

Fig. 7 Measured ignition delay times for lower-concentration $\phi = 1.0$ mixtures (98% Ar) with and without silane.

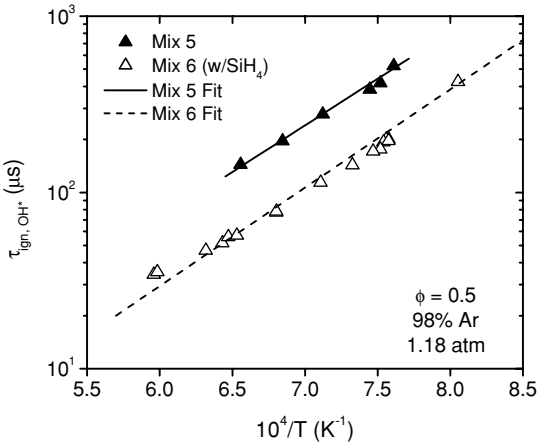

Fig. 8 Measured ignition delay times for lower-concentration $\phi = 0.5$ mixtures (98% Ar) with and without silane.

1300 K. Mixture 3 had a 360-ppm level of SiH_4 or about 7% of the ethylene concentration. The results of the fuel-lean experiments (mixtures 5 and 6) are presented in Fig. 8. In this series of experiments, the addition of 360 ppm silane in mixture 6 constituted about 12% of the C_2H_4 concentration in the mixture. This level of silane addition resulted in a τ_{ign} reduction of about 55% that was fairly constant with temperature. Finally, a plot of the lower-dilution $\phi = 0.5$ data (mixture 7) is provided as Fig. 9.

Each situation in Figs. 6–9 has a unique ignition delay time trend. The data in each of the four log graphs at the higher temperatures

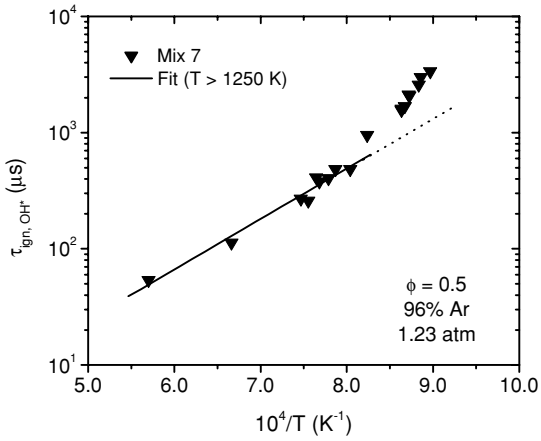

Fig. 9 Measured ignition delay times for higher-concentration $\phi = 0.5$ mixture (96% Ar).

appear to be linear; however, it should not be assumed that the log of the ignition delay time is linear for all temperature regions. Special attention should be paid to the low-temperature regions, where the τ_{ign} seems to deviate from linearity. This trend is particularly evident for the fuel-lean data of mixture 7 in Fig. 9, where there is a clear change in slope for temperatures less than approximately 1250 K.

Correlations of the ignition delay times in Figs. 6–9 were obtained following the usual form for shock-tube ignition delay time data. These correlations are displayed as solid lines for the ethylene-only mixtures and as dashed lines for the mixtures with silane, with excellent agreement in general. The slope of each line on a $\ell_n(\tau_{ign})$ plot is equivalent to E/R, with E being an ignition activation energy and R the universal gas constant. The resulting activation energies are listed for each mixture in Table 1. They range from 20.1 kcal/mol for mixture 7 to 28.9 kcal/mol for mixture 3. The concentration ranges and the temperature ranges of the correlations are also provided in Table 1.

Discussion of Results

Most previous studies of ethylene ignition were able to combine all of the data into a master correlation based on the ignition activation energy and the component concentrations.[19] In similar fashion, the high-temperature ethylene τ_{ign} data of this study (without SiH_4) can be correlated by the following:

$$\tau_{ign} = 3.3 \times 10^{-7}[C_2H_4]^{0.19}[O_2]^{-0.95}[Ar]^{0.04}\exp(26{,}600/RT)$$

In the preceding relation, the ignition time is in μs, the concentrations are in mol/cm^3, R is equal to 1.986 cal/mol-K, and T is the temperature in K. The effect of argon dilution is almost negligible, and the overall pressure dependence from the concentrations is $P^{-0.72}$. Figure 10 presents a plot of the preceding correlation in comparison with the experimental data; the r^2 is 0.96.

A similarly excellent correlation was obtained for the mixtures containing silane ($r^2 = 0.97$). However, the variation in SiH_4 concentration was relatively narrow, and so the concentration exponents are not comparable to the preceding relation for mixtures without silane. The authors feel that the correlation with silane cannot be extrapolated much beyond the conditions of the present study, and so the complete correlation is not presented herein. However, the ignition activation energy for the mixtures with silane (i.e., 26.3 kcal/mol, Table 1) is realistic. This overall value for E is quite close to that obtained without SiH_4, indicating that the small additions of silane, although greatly reducing the ignition delay time, did not appreciably change the overall ethylene chain-branching kinetics at higher temperatures. These results are in contrast with the previous results from the authors' laboratory concerning the addition of silane to C_2H_2 mixtures[35] but are in agreement with the results seen in H_2- and CH_4-based mixtures.[34] For the stoichiometric C_2H_2 mixtures, silane greatly increased the ignition activation energy (from 14.7 to 24 kcal/mol) over a similar concentration range.[35]

Table 3 Survey of ignition activation energies for previous experimental research on ethylene combustion

Other works	E, kcal/mol	T, K
Baker and Skinner[1]	34.2	1058–1876
Colket and Spadaccini[3]	35.0	1125–1410
Drummond[6]	29.5	1090–1630
Gay et al.[7]	24.0	1500–2300
Hidaka et al.[9]	27.5	1400–2100
Homer and Kistiakowsky[10]	17.1	1500–2300
This study	26.6	1223–1746

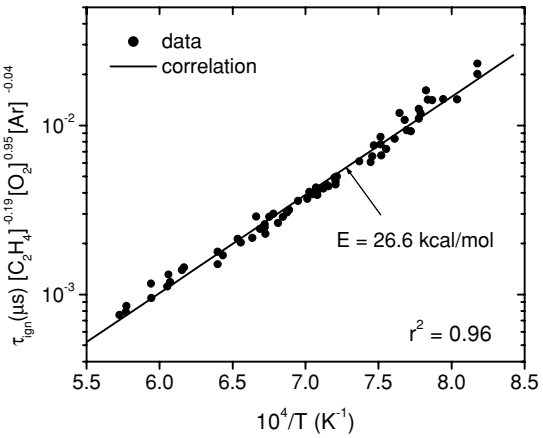

Fig. 10 Overall correlation and experimental data for all mixtures without silane.

It is useful to compare the current ethylene-only ignition activation energies with the results of previous studies. Table 3 presents such a comparison; the wide range of activation energies in the previous studies is apparent but might be caused by the different ranges in temperature, stoichiometry, and concentration of each study. Hence, the established E values are not necessarily incorrect and must be considered on a case-by-case basis. Nonetheless, the present value of 26.6 kcal/mol agrees most closely with the results of Hidaka et al.[9] (27.5 kcal/mol). This agreement is also evident in Fig. 4.

Although a shift in kinetics at intermediate temperatures and higher pressures from chain branching to chain termination has been observed in H_2/O_2 mixtures and some hydrocarbons,[34,35,38] little specific mention has been made in the literature to this effect on C_2H_4 oxidation, although some of the data of previous works do show some indication of it by inspection. However, such a shift is clearly seen in the fuel-lean ignition data of mixture 7 (Fig. 9). The increase in slope is apparent for temperatures less than about 1250 K for this mixture, particularly when contrasted with the slope of the ignition delay times from the higher temperature range. Similar effects are seen at lower temperatures in a few points from the other mixtures, but not enough lower-temperature data are available for these mixtures to be conclusive. The ability of chemical kinetics models to pick up this curvature in τ_{ign} data on an Arrhenius plot is discussed in the following section.

Kinetics Modeling

The data presented herein can provide fundamental validation for research in the area of hydrocarbon ignition and oxidation with trace quantities of silane. Thus, the extent to which these data can serve as useful validation is an important consideration and can first be demonstrated by modeling the mixtures that do not contain silane. Results from mixtures containing silane can then be compared to the predictions of a new mechanism that includes both hydrocarbon and silane kinetics. Many mechanisms exist for the simpler case of C_xH_y oxidation, among which enough discrepancies exist to warrant attention.

With this in mind, a number of modern, detailed chemical kinetics mechanisms have been run over the range of conditions studied experimentally. Results presented are from five such mechanisms, which follow: a high-temperature model of acetylene and ethylene oxidation by Wang and Laskin[40,§]; two mechanisms for higher-order hydrocarbon combustion from Lawrence Livermore National Laboratories—one by Curran et al.[41] for heptane oxidation at high temperatures and one by Marinov et al.[13] for rich, sooting butane flames; a model of methane oxidation at lower temperatures ($700 < T < 1500$ K) by Bendtsen et al.[42] and Glarborg et al.[43] with additional reactions for C_2H_x and NO_x compounds; and finally, a general mechanism of hydrocarbon combustion developed at the University of California San Diego, per Li and Williams.[44,¶]

The choice of mechanisms was based on relevance to the experimental conditions. Other mechanisms were used also, but are not shown because they do not relate to the compounds and conditions of interest (i.e., high-temperature oxidation of ethylene.) Two additional mechanisms are available from Wang and Laskin,[45] which was compiled primarily for acetylene, and Ref. 21 dealing with polycyclic-aromatic-hydrocarbon (PAH) formation. Both gave results similar to those of Ref. 40, but Wang and Laskin's most recent effort[40] was intended specifically for high-temperature C_2H_2 and C_2H_4 oxidation, and in general, showed the best agreement of the three with the present experimental results. The well-known GRI-Mech 3.0[**] showed fair agreement with current results, although calculated ignition delay times were generally faster than the data, and its predictions were similar (within an order of magnitude) to those of the San Diego Mechanism.[44,¶]

All simulations were performed with the Shock routine of the *Chemkin Collection*,[46] and reactions for the formation and quenching of OH* were added to enable direct comparison to the experimental results. As described in Hall et al.,[36] OH* formation was modeled by two main pathways. The first, studied extensively in H_2O_2 mixtures by Petersen et al.,[47] is

$$H + O + M \leftrightarrows OH^* + M \qquad \text{(R1)}$$

The second pathway is the primary formation step in hydrocarbon mixtures and has been studied by Hall and Petersen[48]:

$$CH + O_2 \leftrightarrows OH^* + CO \qquad \text{(R2)}$$

Reactions of the form[49–51]

$$OH^* + M \leftrightarrows OH + M \qquad \text{(R3–13)}$$

described the collisional quenching kinetics, with H_2O and Ar being the dominant quenching molecules because of their high concentrations. The complete set of reactions and their associated rate coefficients can be found in Table 4. A study to optimize these parameters for shock-tube applications is currently underway.[52] Because the electronically excited OH* molecules are present in such small concentrations ($[OH^*]_{max} \approx 10^{-9}$ mol/cm^3 or less—about one million times less than the concentration of its ground-state counterpart, OH), their reactions do not affect the oxidation kinetics of the detailed mechanisms, in fact, order-of-magnitude uncertainties in the OH* reaction rates affect only the absolute concentration formed and have a negligible effect on the time of OH* arrival. Hence, addition of these reactions ensures that no error is introduced by inconsistent diagnostics.

After developing a suitable model of OH* kinetics in the presence of hydrocarbons, an investigation of several detailed kinetics mechanisms was conducted for comparison to the OH* measurements presented thus far. The mechanisms are first tested quantitatively for their ability to predict τ_{ign} as a function of inverse temperature, shown in Figs. 11–14. Then, Figs. 15–17 provide a qualitative evaluation of the five models in the form of species profiles, showing predicted concentrations as functions of time. Only the ability of the individual models to predict the results of the shock-tube experiments are examined; ignition times and species profiles from

¶Data available online at http://maemail.ucsd.edu/combustion/cermech/olderversions/.

**Data available online at http://www.me.berkeley.edu/gri-mech/.

Table 4 OH* submechanism[a]

No.	Reaction	A	n	E	Source
1	$H + O + M \leftrightarrows OH^* + M$	6.00×10^{14}	0.0	6940	Petersen et al.[47]
2	$CH + O_2 \leftrightarrows OH^* + CO$	4.04×10^{13}	0.0	0.0	Hall and Petersen[48]
3	$OH^* + Ar \leftrightarrows OH + Ar$	2.17×10^{10}	0.5	2060	Paul et al.[51]
4	$OH^* + H_2O \leftrightarrows OH + H_2O$	5.92×10^{12}	0.5	−861	Smith et al.[49]
5	$OH^* + CO_2 \leftrightarrows OH + CO_2$	2.75×10^{12}	0.0	−968	Smith et al.[49]
6	$OH^* + CO \leftrightarrows OH + CO$	3.23×10^{12}	0.5	−787	Smith et al.[49]
7	$OH^* + H \leftrightarrows OH + H$	1.50×10^{12}	0.5	0.0	Hidaka et al.[50]
8	$OH^* + H_2 \leftrightarrows OH + H_2$	2.95×10^{12}	0.5	−444	Smith et al.[49]
9	$OH^* + O_2 \leftrightarrows OH + O_2$	2.10×10^{12}	0.5	−482	Smith et al.[49]
10	$OH^* + O \leftrightarrows OH + O$	1.50×10^{12}	0.5	0.0	Hidaka et al.[50]
11	$OH^* + OH \leftrightarrows OH + OH$	1.50×10^{12}	0.5	0.0	Hidaka et al.[50]
12	$OH^* + CH_4 \leftrightarrows OH + CH_4$	3.36×10^{12}	0.5	−635	Smith et al.[49]
13	$OH^* \leftrightarrows OH + h\nu$	1.40×10^{6}	0.0	0.0	Hidaka et al.[50]

[a]Reactions were added to each detailed mechanism to match the experimental diagnostics. Rate coefficients are given by $k = AT^n \exp(-E/RT)$ in cm, mol, cal units.

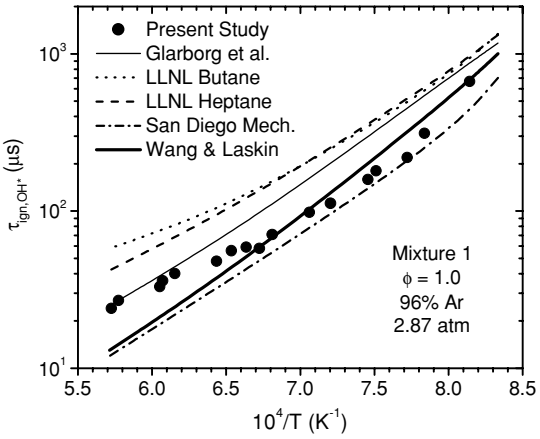

Fig. 11 Ignition delay time curves by several mechanisms: low-dilution, high-pressure stoichiometric case.

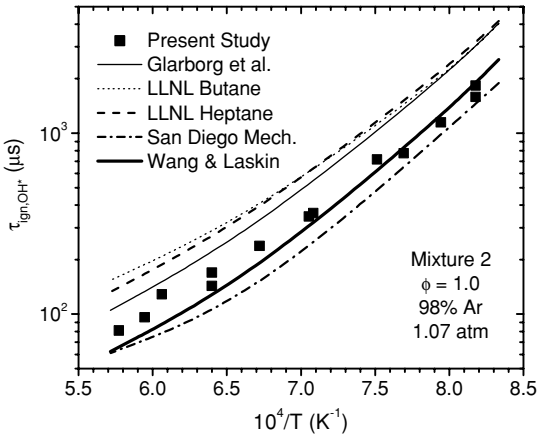

Fig. 12 Ignition delay time curves by several mechanisms: high-dilution, atmospheric pressure, stoichiometric case.

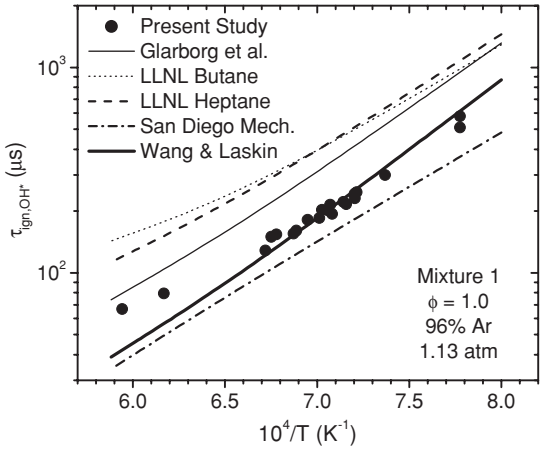

Fig. 13 Ignition delay time curves by several mechanisms: low-dilution, atmospheric pressure, stoichiometric case.

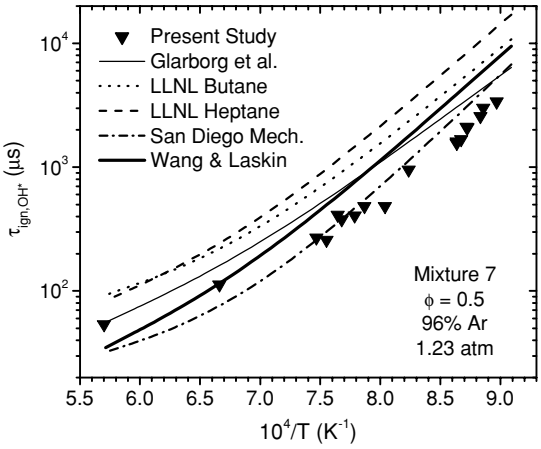

Fig. 14 Ignition delay time curves by several mechanisms: fuel-lean, low-dilution case.

shock-tube experiments alone are not sufficient to validate a particular mechanism.

Ignition Times

In this section, modern kinetics mechanisms are tested for their ability to predict ignition delay relative to some initial time. The precise measurement of such delays is a unique advantage of shock-tube studies, which provide uniform heating of the test area to energy levels in excess of the activation energy and do so in a manner that is practically instantaneous. It is known that the plethora of combustion intermediates whose advent characterizes the induction zone all form around the same time, and it is this time that is commonly termed "ignition." For this study, the intermediate of choice is the electronically excited OH* whose presence was monitored in the shock-tube experiments, so that the time to OH* formation characterizes the mechanism's prediction of ignition time, without regard for the nature or extent of the combustion process.

The mechanisms are generally able to predict the activation energy of the overall reaction as can be seen from the slope of each curve on the τ_{ign} plots. Trends in variation of model from experiment are fairly consistent across all conditions considered. Wang and Laskin[40,§] predict the experimental delay time typically within 10%,

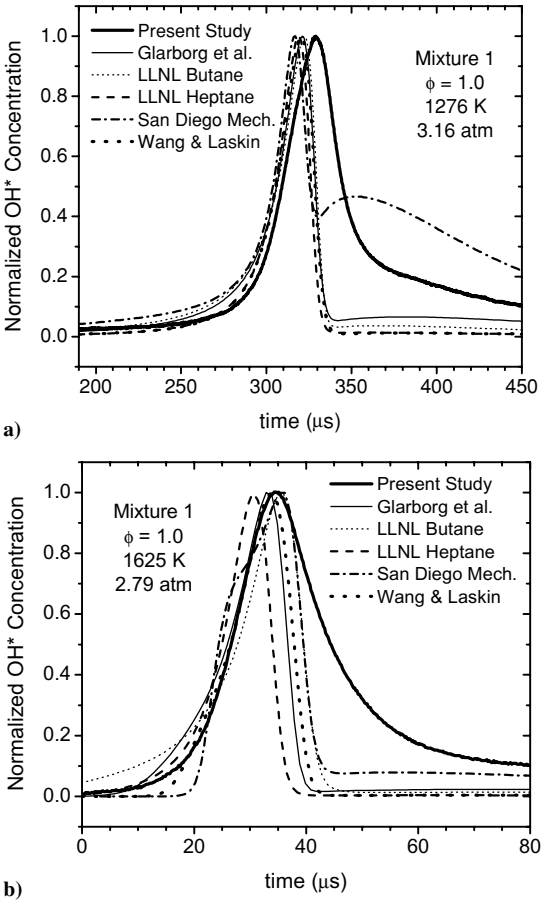

Fig. 15 Species profiles for mixture 1 ($\phi = 1.0$, 96% Ar) near 3 atm by several mechanisms: a) low temperature (1276 K) and b) high temperature (1625 K).

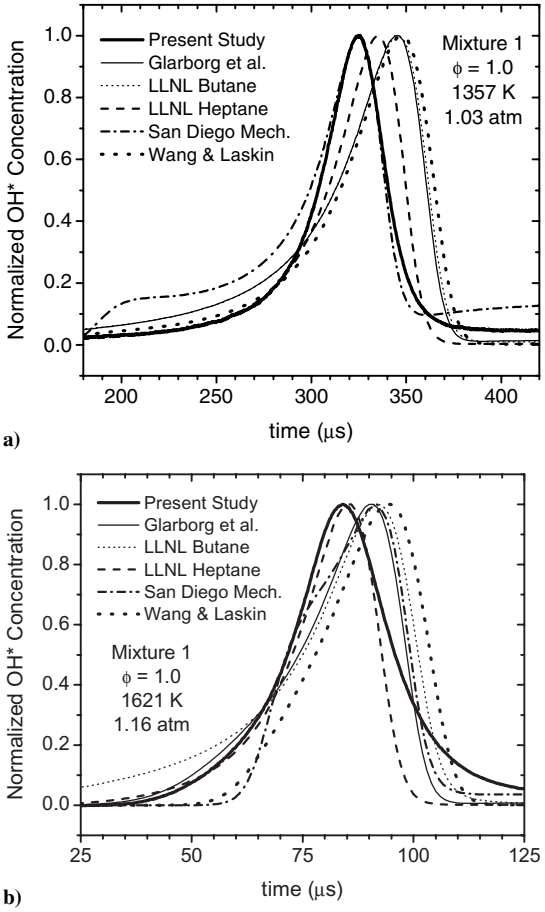

Fig. 16 Species profiles for mixture 1 ($\phi = 1.0$, 96% Ar) near 1 atm by several mechanisms: a) low temperature (1357 K) and b) high temperature (1621 K).

showing errors of at most 50%. The San Diego Mechanism[44,¶] predicts ignition that is either faster than experiment by about 30%, or is within 10% of the experimental value, and hence within the scatter of the data themselves. The model by Bendtsen et al.[42] and Glarborg et al.[43] overpredicts the ignition delay by as much as 50%, although, as can be seen in Figs. 12 and 14, its agreement is often closer to 25%. The Lawrence Livermore National Laboratories (LLNL) butane mechanism[13] shows error approaching a factor of 2, and even exceeding such error in the high-temperature regime (e.g., Fig. 13, $T > 1550$ K). The error committed by the LLNL Heptane mechanism is typically within a factor of two and is slower than the data.

The low-temperature shift in activation energy seen in Figs. 11 and 14 is an important aspect of the kinetics and offers an interesting test of the models. An upward curvature (i.e., increased activation energy) can be seen at lower temperatures ($T < 1250$ K) in the predictions of Wang and Laskin and of the San Diego Mechanism in Figs. 12 and 14. Although not shown here, the two other models by Wang and Frenklach[21] and Wang and Laskin[45] displayed the curvature of Fig. 14 even better than the one shown. This was the only case in which the models of C_2H_2 oxidation[45] and PAH formation[21] matched experimental results better than did the C_2H_2/C_2H_4 model.[40,§] The C_2H_2/C_2H_4 model was selected to represent the three mechanisms by Wang et al. because of its superior performance on the remaining three mixtures without SiH_4 and because of its applicability to C_2H_4 combustion in particular.

The mechanism by Bendtsen et al.[42] and Glarborg et al.[43] does not display this low-temperature shift in kinetics, at least not in the temperature range considered in this study. This model has been found to predict a straight-line τ_{ign} curve (on an Arrhenius plot) with the possible exception of Fig. 12, where it shows slight curvature. One possible reason for this linear behavior is that its calibration temperatures were on the order of 700–1300 K, which is considered low for shock-tube studies. Hence, if such a trend were to be seen, it could be expected in the low-temperature regime of the flow reactor studies upon which that model was based.[43] The LLNL Butane model[13] does show a greater activation energy at lower temperatures, with an inflection point in its τ_{ign} curve near 1450 K in each case. The LLNL heptane model exhibited linear behavior over the entire range of conditions considered. Notably, in the C_2H_2 case,[35] where this low-temperature shift was also observed, both mechanisms from Lawrence Livermore National Laboratories followed the trend well, although they were offset from the experimental curve, predicting faster ignition.

Species Profiles

Another advantage of shock-tube studies is the constant, uniform distribution of properties throughout the test section for the duration of the test time (assuming a sufficiently large inner diameter). Measurements of emission intensity as a function of time are directly proportional to the concentration of the emitting species (in this case OH^*), and these data (i.e., concentration vs time at an arbitrary point in the test section) are comparable to the mechanism output so that the species profile shapes can be compared directly. For comparison, all curves have been normalized to their maximum values and offset to the experimental delay time to isolate the curves' shapes.

Figure 15 shows species profiles from the stoichiometric mixture that was tested at higher pressure for comparison to other studies. At these pressures (about 3 atm), the models tend to display narrow profiles compared to the data. An important feature of the kinetics is the postignition duration of OH^* (e.g., Fig. 15a near 500 μs). These conditions gave rise to the continued presence of OH^* (about 5–10% of its peak value) for at least several hundred μs after the rapid, postpeak decrease typical of all OH^* profiles. This trend can be seen in the predictions of Bendtsen et al.[42] and Glarborg et al.[43] and the San Diego Mechanism[44,¶] although they differ in magnitude.

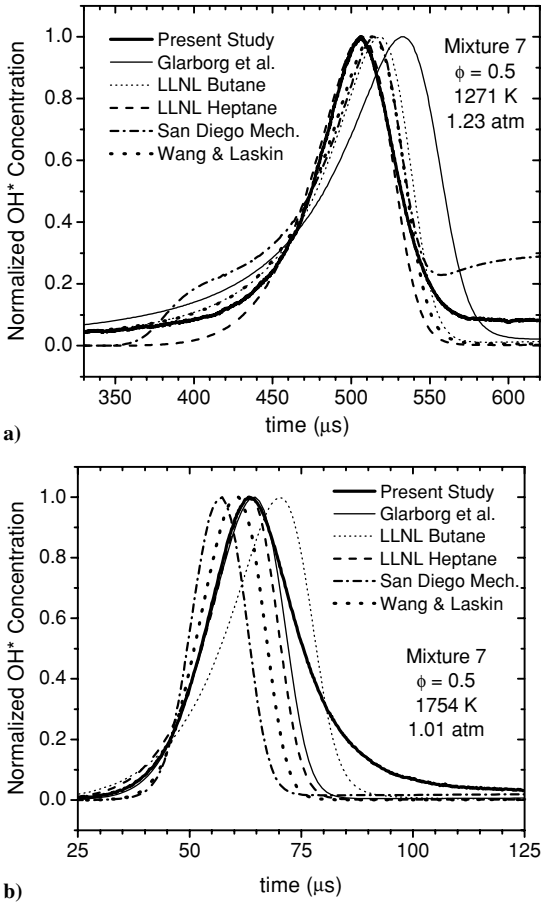

Fig. 17 Species profiles for mixture 7 ($\phi = 0.5$, 96% Ar) near 1 atm by several mechanisms: a) low temperature (1271 K) and b) high temperature (1754 K).

Experimental data from both the high- and low-temperature cases show a gradual increase in radical concentration before ignition; this trend is also shown by the models, but not exactly.

Typical results for the stoichiometric data at near-atmospheric pressures are shown in Fig. 16. Agreement of model with experiment is good at these conditions, especially regarding the width of the OH* profile. One important difference can be seen in Fig. 16a, wherein the San Diego Mechanism[44,¶] overpredicts the preignition rise and the postignition duration. This is likely because of the low CH concentration predicted by that model. CH is known to be the primary precursor for OH* via R2, with secondary formation from R1. Thus, with low levels of CH formed, the contribution from R1 before and after ignition is large by comparison.

For the low-temperature case (Fig. 16a) all models agree reasonably well. The LLNL heptane mechanism follows the data most closely in terms of profile shape, whereas the other models show a more gradual ignition rise. In the high-temperature case (Fig. 16b), there is some disagreement among the mechanisms concerning the initial rise time and the slope of the ignition curve; once again, the LLNL heptane mechanism follows these trends most closely.

Regarding the two lean mixtures, the models predict the experimental emission very well—perhaps even better than for stoichiometric conditions. The only major deviation can be seen in Fig. 17a, where at low temperatures the San Diego Mechanism overpredicts the preignition rise. This is noteworthy because the data do show such a rise but differ in magnitude. Of particular interest is the fact that the most of the mechanisms predict some sort of preignition increase in OH*, which is so prominent in the data. Although some improvement in this area is still needed, the fact that the models predict this behavior points to the preignition rise in OH* being a kinetic phenomenon and not an artifact of the experiment. In the fuel-lean, high-temperature cases, for example Fig. 17b, all models reproduced the data reasonably well.

Although some important deviations have been noted, the mechanisms are generally able to predict the shape of the OH* concentration curve. This is significant at times when additional information is needed regarding the entire combustion process besides simply the delay time. This also suggests that the reactions added to model the excited state radical are sufficient, although further improvements are possible in the future, for both the OH* kinetics and the detailed mechanisms.

Silane Kinetics

To elucidate the effect of silane addition on ethylene ignition as observed experimentally, a preliminary mechanism for the ignition of C_2H_X fuels in the presence of silane was assembled from the hydrocarbon mechanism of Wang and Laskin[40] and the SiH_4 mechanism of Miller et al.[53] In the stoichiometric case (mixtures 2 and 3), the model shows excellent agreement with the experimental ignition times, matching the slopes of both curves as well as their magnitude. In the fuel-lean case (mixtures 5 and 6), the new model is again able to reproduce the reduction in ignition time caused by silane addition and the slope of both curves. These promising results suggest that the model contains the important oxidation pathways and can provide additional insights regarding the mechanisms by which small amounts of silane can significantly reduce the ignition-delay time of ethylene mixtures. A more comprehensive study of the silane/hydrocarbon kinetics is beyond the scope of this paper and is presented elsewhere.[54]

Conclusions

Ethylene combustion is of interest because of its many applications in the combustion sciences, and the interaction of C_2H_4 with silane is of particular interest for advanced-propulsion and materials science applications. For these reasons, four mixtures composed of $C_2H_4/O_2/Ar$ and three mixtures consisting of $C_2H_4/O_2/Ar/SiH_4$ were reacted behind reflected shock waves in a shock tube in the temperature range 1115–1900 K at pressures near either 1 or 3 atm. There were several purposes to these experiments: 1) to observe and measure the ignition delay time behavior with and without silane addition at elevated temperatures; 2) to establish a database of characteristic times and species profiles for comparison to chemical kinetics models for their validation and improvement; 3) to compare the results to previous experimental data on C_2H_4 ignition; and 4) to outline by example a methodology for interpreting and analyzing shock-tube ignition and oxidation studies.

The benefits of silane addition to C_2H_4 combustion were examined, and even very small amounts of silane ($<10\%$ of fuel concentration) were seen to reduce the ignition delay times by as much as 50% in some cases. The overall activation energy for the higher temperatures (>1250 K) was found to be 26.6 kcal/mol for the mixtures without SiH_4 and 26.3 kcal/mol for the mixtures with SiH_4.

Several modern, detailed chemical kinetics mechanisms including reactions for ethylene oxidation were compared to the ignition-time and OH* time-history data for the mixtures without silane. To obtain the best agreement with the experimental results, a submechanism that handles the formation and quenching of electronically excited hydroxyl (OH^*) was added to each base mechanism because OH* was the species measured in the experiments. Most mechanisms were able to reproduce the trend in ignition in terms of its activation energy, but the Wang and Laskin model[40,§] in particular was able to also match the absolute τ_{ign} within (usually) 10% for the entire range of mixtures and conditions of the experiment. Direct comparisons were also made to normalized OH* profiles with the general result being that the basic shapes of the profiles were captured in most cases. However, some improvement is still necessary in all mechanisms to capture some of the subtleties in the experimental profiles for the entire data set.

Acknowledgments

This work was supported by The Aerospace Corporation and the Air Force Space and Missile Systems Center under Contract F04701-00-C-0009 and by the University of Central Florida (UCF).

The authors wish to thank Carrol Gardner (Aerospace) and Matthew Rickard (Aerospace) for their invaluable assistance in the laboratory and Schuyler Smith and Allison Kraft (UCF) for assistance with the calculations. Personnel communications with Professor Williams and Maria Petrova at the University of California San Diego provided helpful insights in interpretation of their kinetics mechanism.

References

[1]Baker, J., and Skinner, G., "Shock-Tube Studies on the Ignition of Ethylene-Oxygen-Argon Mixtures," *Combustion and Flame*, Vol. 19, No. 3, 1972, pp. 347–350.

[2]Brown, C., and Thomas, C., "Experimental Studies of Shock-Induced Ignition and Transition to Detonation in Ethylene and Propane Mixtures," *Combustion and Flame*, Vol. 117, No. 4, 1999, pp. 861–870.

[3]Colket, M., and Spadaccini, L., "Scramjet Fuels Autoignition Study," *Journal of Propulsion and Power*, Vol. 17, No. 2, 2001, pp. 315–323.

[4]Dagaut, P., Voisin, D., Cathonnet, M., McGuinness, M., and Simmie, J., "The Oxidation of Ethylene Oxide in a Jet-Stirred Reactor and Its Ignition in Shock Waves," *Combustion and Flame*, Vol. 106, No. 1–2, 1996, pp. 62–68.

[5]Dagaut, P., Boettner, J.-C., and Cathonnet, M., "Ethylene Pyrolysis and Oxidation: A Kinetic Modeling Study," *International Journal of Chemical Kinetics*, Vol. 22, No. 6, 1990, pp. 641–664.

[6]Drummond, L., "Shock-Initiated Exothermic Reactions: The Oxidation of Ethylene," *Australian Journal of Chemistry*, Vol. 21, No. 3, 1968, pp. 2641–2648.

[7]Gay, I., Glass, G., Kern, R., and Kistiakowsky, G., "Ethylene-Oxygen Reaction in Shock Waves," *Journal of Chemical Physics*, Vol. 47, No. 1, 1967, pp. 313–320.

[8]Hidaka, Y., Nishimori, T., Sato, K., Henmi, Y., Okuda, R., and Inami, K., "Shock-Tube and Modeling Study of Ethylene Pyrolysis and Oxidation," *Combustion and Flame*, Vol. 117, No. 4, 1999, pp. 755–776.

[9]Hidaka, Y., Kataoka, T., and Suga, M., "A Shock-Tube Investigation of Ignition in Ethylene-Oxygen-Argon Mixtures," *Bulletin of the Chemical Society of Japan*, Vol. 47, No. 9, 1974, pp. 2166–2170.

[10]Homer, J., and Kistiakowsky, G., "Oxidation and Pyrolysis of Ethylene in Shock Waves," *Journal of Chemical Physics*, Vol. 47, No. 12, 1967, pp. 5290–5295.

[11]Jachimowski, C., "An Experimental and Analytical Study of Acetylene and Ethylene Oxidation Behind Shock Waves," *Combustion and Flame*, Vol. 29, Jan. 1977, pp. 55–66.

[12]Lutz, A., Kee, R., Miller, J., Dwyer, H., and Oppenheim, A., "Dynamic Effects of Autoignition Centers for Hydrogen and $C_{1,2}$-Hydrogen Fuels," *Proceedings of the Combustion Institute*, Vol. 22, 1988, pp. 1683–1693.

[13]Marinov, N., Pitz, W., Westbrook, C., Vincitore, A., Castaldi, M., Senkan, S., and Melius, C., "Aromatic and Polycyclic Aromatic Hydrocarbon Formation in a Laminar Premixed n-Butane Flame," *Combustion and Flame*, Vol. 114, No. 1–2, 1998, pp. 192–213.

[14]Montgomery, C., Zhao, W., Adams, B., Eklund, D., and Chen, J., "CFD Simulations of Supersonic Combustion Using Reduced Chemical Kinetic Mechanisms and ISAT," AIAA Paper 2003-3547, June 2003.

[15]Schultz, E., and Shepherd, J., "Validation of Detailed Reaction Mechanisms for Detonation Simulation," Explosion Dynamics Lab., GALCIT, California Inst. of Technology, Pasadena, CA, Rept. FM99-5, 2000.

[16]Skinner, G., Sweet, R., and Davis, S., "Shock-Tube Experiments on the Pyrolysis of Deuterium-Substituted Ethylenes," *Journal of Physical Chemistry*, Vol. 75, No. 1, 1971, pp. 1–12.

[17]Suzuki, M., Moriwaki, T., Okazaki, S., Okuda, T., and Tanzawa, T., "Oxidation of Ethylene in Shock-Tube," *Acta Astronautica*, Vol. 18, Nov. 1971, pp. 359–365.

[18]Tan, Y., Dagaut, P., Cathonnet, M., Boettner, J., Bachman, J., and Carlier, P., "Natural Gas and Blends Oxidation and Ignition; Experiments and Modeling," *Proceedings of the Combustion Institute*, Vol. 25, 1994, pp. 1563–1569.

[19]Varatharajan, B., and Williams, F., "Ethylene Ignition and Detonation Chemistry, Part 1: Detailed Modeling and Experimental Comparison," *Journal of Propulsion and Power*, Vol. 18, No. 2, 2002, pp. 344–351.

[20]Varatharajan, B., and Williams, F., "Ethylene Ignition and Detonation Chemistry, Part 2: Ignition Histories and Reduced Mechanisms," *Journal of Propulsion and Power*, Vol. 18, No. 2, 2002, pp. 352–362.

[21]Wang, H., and Frenklach, M., "Detailed Kinetic Modeling Study of Aromatics Formation in Laminar Premixed Acetylene and Ethylene Flames," *Combustion and Flame*, Vol. 110, No. 1–2, 1997, pp. 173–221.

[22]McLain, A. G., Jachimowski, C. J., and Rogers, R. C., "Ignition of SiH_4-H_2-O_2-N_2 Behind Reflected Shock Waves," NASA Technical Paper 2114, Feb. 1983.

[23]Golovitchev, V. I., and Bruno, C., "Numerical Study of the Ignition of Silane/Hydrogen Mixtures," *Journal of Propulsion and Power*, Vol. 15, No. 1, 1998, pp. 92–96.

[24]Lewis, M. J., and Chang, J. S., "Joint Jet-A/Silane/Hydrogen Reaction Mechanism," *Journal of Propulsion and Power*, Vol. 16, No. 2, 2000, pp. 365–367.

[25]Takahashi, T., Hagiwara, K., Egashira, Y., and Komiyama, H., "The Effect of Gas-Phase Additives C_2H_4, C_2H_6, and C_2H_2 on SiH_4/O_2 Chemical Vapor Deposition," *Journal of the Electrochemical Society*, Vol. 143, No. 4, 1996, pp. 1355–1361.

[26]Kondo, S., Tokuhashi, K., Nagai, H., Iwasaka, M., and Kaise, M., "Experimental Study of Spontaneous Ignition Limit of Oxygen-Lean Silane Mixtures," *Combustion and Flame*, Vol. 97, No. 3–4, 1994, pp. 296–300.

[27]Koda, S., "Kinetic Aspects of Oxidation and Combustion of Silane and Related Compounds," *Progress in Energy and Combustion Science*, Vol. 18, No. 6, 1992, pp. 513–528.

[28]Wooldridge, M. S., "Gas-Phase Combustion Synthesis of Particles," *Progress in Energy and Combustion Science*, Vol. 24, No. 1, 1998, pp. 63–87.

[29]Woiki, D., Catoire, L., and Roth, P., "High-Temperature Kinetics of Si-Containing Precursors for Ceramic Processing," *AIChE Journal—Ceramics Processing 1997*, Vol. 43, No. 11A, 1997, pp. 2670–2678.

[30]Pratsinis, S. E., "Flame Aerosol Synthesis of Ceramic Powders," *Progress in Energy and Combustion Science*, Vol. 24, No. 3, 1998, pp. 197–219.

[31]Chung, S.-L., and Katz, J. L., "The Counterflow Diffusion Flame Burner: A New Tool for the Study of Nucleation of Refractory Compounds," *Combustion and Flame*, Vol. 61, No. 3, 1985, pp. 271–284.

[32]Erwin, J. W., Ring, M. A., and O'Neal, H. E., "Mechanism and Kinetics of the Silane Decomposition in the Presence of Acetylene and in the Presence of Olefins," *International Journal of Chemical Kinetics*, Vol. 17, No. 10, 1985, pp. 1067–1083.

[33]Kalitan, D. M., and Petersen, E. L., "Evaluation of Several Chemical Kinetics Mechanisms of Silane Ignition and Oxidation at Elevated Temperatures," *Combustion and Flame* (submitted for publication).

[34]Petersen, E. L., Kalitan, D. M., and Rickard, M. J., "Reflected-Shock Ignition of $SiH_4/H_2/O_2/Ar$ and $SiH_4/CH_4/O_2/Ar$ Mixtures," *Journal of Propulsion and Power*, Vol. 20, No. 4, 2004, pp. 665–674.

[35]Rickard, M. J. A., Hall, J. M., and Petersen, E. L., "Effect of Silane Addition on Acetylene Ignition behind Reflected Shock Waves," *Proceedings of the Combustion Institute*, Vol. 30, 2005, pp. 1915–1923.

[36]Hall, J. M., Rickard, M. J. A., and Petersen, E. L., "Comparison of Characteristic Time Diagnostics for Ignition and Oxidation of Fuel/Oxidizer Mixtures Behind Reflected Shock Waves," *Combustion Science and Technology*, Vol. 177, No. 3, 2005, pp. 455–483.

[37]Petersen, E. L., Rickard, M. J. A., Crofton, M. W., Abbey, E. D., Traum, M. J., and Kalitan, D. M., "A Facility for Gas- and Condensed-Phase Measurements Behind Shock Waves," *Measurement Science and Technology*, Vol. 16, No. 9, 2005, pp. 1716–1729.

[38]Petersen, E. L., Davidson, D. F., and Hanson, R. K., "Ignition Delay Times of Ram Accelerator CH_4/O_2/Diluent Mixtures," *Journal of Propulsion and Power*, Vol. 15, No. 1, 1999, pp. 82–91.

[39]Horning, D. C., Davidson, D. F., and Hanson, R. K., "Study of the High-Temperature Autoignition of n-Alkane/O_2/Ar Mixtures," *Journal of Propulsion and Power*, Vol. 18, No. 2, 2002, pp. 363–371.

[40]Wang, H., and Laskin, A., "A Comprehensive Kinetic Model of Ethylene and Acetylene Oxidation at High Temperatures," Dept. of Mechanical Engineering, Univ. of Delaware, Internal Report, Newark, 1998.

[41]Curran, H. J., Gaffuri, P., Pitz, W. J., and Westbrook, C. K., "A Comprehensive Modeling Study of Iso-Octane Oxidation," *Combustion and Flame*, Vol. 129, No. 3, 2002, pp. 253–280.

[42]Bendtsen, A. B., Glarborg, P., and Dam-Johansen, K., "Low Temperature Oxidation of Methane: The Influence of Nitrogen Oxides," *Combustion Science and Technology*, Vol. 151, No. 1, 2000, pp. 31–71.

[43]Glarborg, P., Alzueta, M. U., Dam-Johansen, K., and Miller, J. A., "Kinetic Modeling of Hydrocarbon/Nitric Oxide Interactions in a Flow Reactor," *Combustion and Flame*, Vol. 115, No. 1–2, 1998, pp. 1–27.

[44]Li, S. C., and Williams, F. A., "NO_x Formation in Two-Stage Methane-Air Flames," *Combustion and Flame*, Vol. 118, No. 3, 1999, pp. 399–414.

[45]Wang, H., and Laskin, A., "On Initiation Reactions of Acetylene Oxidation in Shock Tubes A Quantum Mechanical and Kinetic Modeling Study," *Chemical Physics Letters*, Vol. 303, No. 1, 1999, pp. 43–49.

[46]Kee, R. J., Rupley, F. M., Miller, J. A., Coltrin, M. E., Grcar, J. F., Meeks, E., Moffat, H. K., Lutz, A. E., Dixon-Lewis, G., Smooke, M. D., Warnatz, J., Evans, G. H., Larson, R. S., Mitchell, R. E., Petzold, L. R., Reynolds, W. C., Caracotsios, M., Stewart, W. E., Glarborg, P., Wang, C., and Adigun, O., *Chemkin Collection*, Release 3.6, Reaction Design, Inc., San Diego, CA, 2000.

[47]Petersen, E. L., Kalitan, D. M., and Rickard, M. J. A., "Calibration and Chemical Kinetics Modeling of an OH Chemiluminescence Diagnostic," AIAA Paper 2003-4493, July 2003.

[48]Hall, J. M., and Petersen, E. L, "Kinetics of OH Chemiluminescence in the Presence of Hydrocarbons," AIAA Paper 2004-4164, July 2004.

[49]Smith, G. P., Luque, J., Park, C., Jeffries, J. B., and Crosley, D. R., "Low Pressure Flame Determinations of Rate Constants for OH(A) and CH(A) Chemiluminescence," *Combustion and Flame*, Vol. 131, No. 1–2, 2002, pp. 59–69.

[50]Hidaka, Y., Takahashi, S., Kawano, H., Suga, M., and Gardiner, W. C., Jr., "Shock Tube Measurement of the Rate Constant for Excited OH ($A^2\Sigma^+$) Formation in the Hydrogen-Oxygen Reaction," *Journal of Physical Chemistry*, Vol. 86, No. 8, 1982, pp. 1429–1433.

[51]Paul, P. H., Durant, J. L., Gray, J. A., and Furlanetto, M. R., "Collisional Electronic Quenching of OH $A^2\Sigma(v' = 0)$ Measured at High Temperature in a Shock Tube," *Journal of Chemical Physics*, Vol. 102, No. 21, 1995, pp. 8378–8384.

[52]Hall, J. M., and Petersen, E. L., "An Optimized Kinetics Model for OH Chemiluminescence at High Temperatures and Atmospheric Pressures," *International Journal of Chemical Kinetics* (to be published).

[53]Miller, T. A., Wooldridge, M. S., and Bozzelli, J. W., "Computational Modeling of the $SiH_3 + O_2$ Reaction and Silane Combustion," *Combustion and Flame*, Vol. 137, No. 1–2, 2004, pp. 73–92.

[54]Hall, J. M., de Vries, J., and Petersen, E. L., "Development of a Chemical Kinetics Mechanism for C_2H_X Ignition in the Presence of Silane," *Proceedings of the 4th Joint Meeting of the U.S. Sections of the Combustion Institute*, 2005.